SIMULATIONS FOR EXPERIMENTAL STUDY OF WARM DENSE MATTER AND INERTIAL FUSION ENERGY APPLICATIONS ON NDCX-II

By
J.J. Barnard, J. Armijo, F.M. Bieniosek, A. Friedman, M. Hay, E. Henestroza, B.G. Logan, R.M. More, P.A. Ni, L.J. Perkins, S-F. Ng, J.S. Wurtele, S.S. Yu, A.B. Zylstra
Lawrence Berkeley National Laboratory
Lawrence Livermore National Laboratory

September 2009

Simulations for experimental study of warm dense matter and inertial fusion energy applications on NDCX-II

J. J. Barnard[1], J. Armijo[2], F. M. Bieniosek[2], A. Friedman[1], M. Hay[2], E. Henestroza[2], B. G. Logan[2], R. M. More[2], P. A. Ni[2], L. J. Perkins[1], S-F. Ng[2,4], J.S. Wurtele[2], S.S. Yu[2,4], A. B. Zylstra[2]

[1]*Lawrence Livermore National Laboratory, Livermore, CA, USA*
[2]*Lawrence Berkeley National Laboratory, Berkeley, CA, USA*
[3]*Tech-X Corporation, Boulder, CO, USA*
[4]*Chinese University, Hong Kong, China*

E-mail: jjbarnard@llnl.gov

Abstract. The Neutralized Drift Compression Experiment II (NDCX II) is an induction accelerator planned for initial commissioning in 2012. The final design calls for a ~3 MeV, ~30 A Li^+ ion beam, delivered in a bunch with characteristic pulse duration of 1 ns, and transverse dimension of order 1 mm. The purpose of NDCX II is to carry out experimental studies of material in the warm dense matter regime, and ion beam/hydrodynamic coupling experiments relevant to heavy ion based inertial fusion energy. In preparation for this new machine, we have carried out hydrodynamic simulations of ion-beam-heated, metallic solid targets, connecting quantities related to observables, such as brightness temperature and expansion velocity at the critical frequency, with the simulated fluid density, temperature, and velocity. We examine how these quantities depend on two commonly used equations of state.

1. Introduction

Ion beams have a number of advantages for heating materials to the Warm Dense Matter (WDM) state [1 - 4]. Included among these are capabilities for spatially uniform and volumetric energy deposition over relatively large and diagnosable material volumes. The Neutralized Drift Compression Experiment (NDCX II) is now being constructed at Lawrence Berkeley National Laboratory to study Warm Dense Matter questions and to investigate target-beam coupling relevant to heavy-ion driven inertial fusion energy. NDCX II is the successor to the experiment NDCX I that demonstrated the technique of injecting plasma into the final beam path to greatly reduce the effects of space charge and therefore achieve short pulses needed for WDM and IFE studies [5]. The physics design of the NDCX II accelerator is described elsewhere [6]. In section 2, we review the target configurations considered for NDCX II. In section 3, we give an example of simulations of a solid Aluminum foil target. In sections 4 and 5, we examine the expected temperature and velocity at the critical surface.

2. Target configurations for NDCX II

A number of target configurations have been considered for NDCX II. These include spherical [7] and cylindrical bubbles [8] (to create enhanced regions of higher pressure and temperature) and planar solid and planar foam [9] targets. Pulse formats include

single pulses of fixed ion energy (but with an energy spread at the target) for WDM studies, and double pulses with varied energy (or single pulses with ion energy that changes over the pulse) to investigate ion-coupling efficiency[10]. Recent heavy ion driven "direct drive" target simulations for inertial fusion energy have shown promisingly high fusion gain [11], by increasing the range over the course of the pulse. This increasing range can be accomplished by increasing the ion energy over the course of the pulse. Experiments that demonstrate increased coupling efficiency, by increasing the range over the course of the pulse, have been simulated[10]. In this paper, however, we focus on the WDM mission for NDCX II.

3. Simulation of beam-heated solid aluminum target

As described in section 2, NDCX II is being designed to heat both solid and porous planar metallic foils, among other options. For the simulations described in this paper we used the radiation hydrodynamics code HYDRA [12]. We assumed the target material was a 3.5 μm thick solid Aluminum, and that the equation of state was either QEOS [13] or LEOS, both of which are accessible by the HYDRA code. The ion intensity varied with time as a parabola of full width duration 1 ns. The ion beam used was a 2.8 MeV Li$^+$ beam and the simulation used HYDRA's Bethe-Bloch ion deposition algorithm. The intensity was adjusted to yield approximately 20 kJ/g integrated over the pulse. The HYDRA simulations were 2D with an assumed 0.5 mm beam radius; the results here simply describe the 1D evolution of the target along the longitudinal axis (parallel to the beam direction). Figure 1 describes the evolution of the density, temperature, velocity, and charge state Z* of the target during the 1 ns of heating of the pulse.
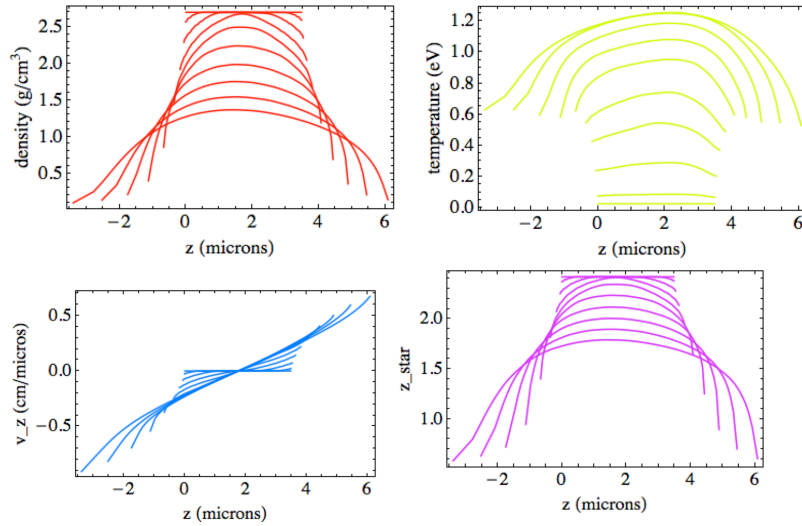

Figure 1. Longitudinal variation of target at radial center (r=0) for ten different times equally spaced between 0 and 1 ns. Ion beam heating ends at 1 ns. Target initially lies between 0 and 3.5 microns. Upper left: Density vs. longitudinal distance z; Upper right: Temperature kT vs. z. Lower left: Longitudinal velocity v_z vs. z; Lower right: Effective charge state of target Z* vs. z.

4. Predicted brightness temperature evolution for beam heated Aluminum target

For the target described in section 3, with finite initial temperature non-uniformity, using either QEOS or LEOS as the equation of state, and an evolving Z*, the

evolution will differ from that described in section 4. As a way of testing the ability of pyrometer measurements [14] to discriminate equations of state in an actual experiment, we estimated the temperature as a function of time as measured by a pyrometer at three widely separated wavelengths, using the ion pulse parameters and two EOS's described in section 3. For the brightness temperature, we assume the following a simple model for the brightness temperature T_b: $T_b = T_{max}$ if $\nu > \nu_{critmax}$; $T_b = T(\nu_{crit})$ if $\nu_{critmax} > \nu > \nu_{critmin}$, and 0 if $\nu_{critmin} > \nu$. Here T_{max} is the maximum material temperature within the foil (generally found at the foil center), $\nu_{critmax}$ is the maximum critical frequency in the foil (also usually at the center) and $\nu_{critmin}$ is the minimum critical frequency in the simulation (usually at the outermost zone, numerically limited by the finite density of the lagrangian fluid element). The results for the NDCX II simulations are found in figs. 4 and 5.
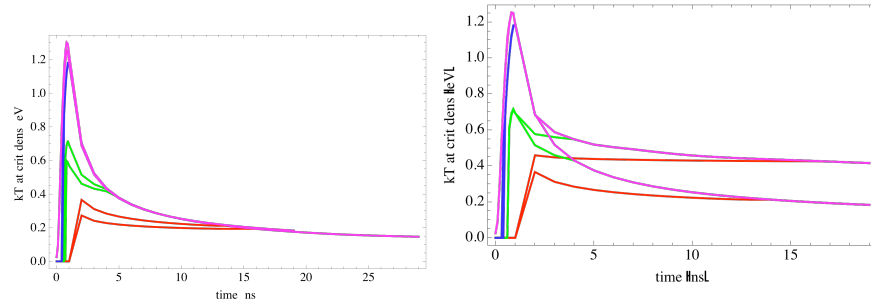

Figure 2. Left: Evolution of brightness temperature (defined in eq. 3) for three observation photon energies (red: 1500 nm; green 450 nm, and blue: 150 nm) and two equations of state (upper: LEOS; lower: QEOS). Both EOS are without Maxwell construction. The magenta curve is the evolution of T_{max}. Right: Same as left figure, except that the upper curves are LEOS without Maxwell construction, and the lower curves are with the Maxwell construction.

5. Predicted velocity evolution for beam heated Aluminum target

We may similarly calculate the velocity that would be inferred by a reflected laser pulse if the reflection occurs predominantly at the critical frequency. These results are shown in figure 4.
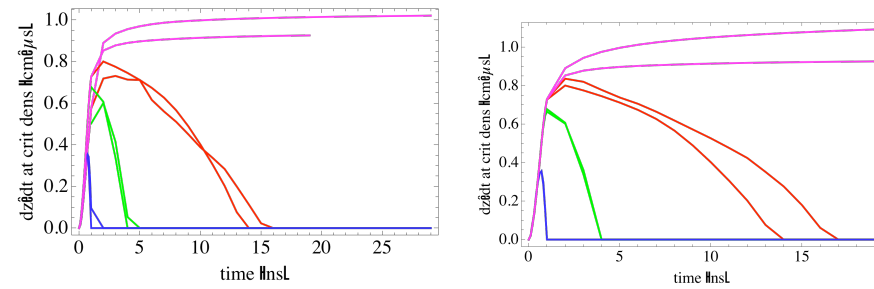

Figure 3. Left: Evolution of velocity at the critical density for three observation photon energies (red: 1500 nm; green 450 nm, and blue: 150 nm) and two equations of state (upper: LEOS; lower: QEOS). Both EOS are without Maxwell construction. The magenta curve is the evolution of v_{max}, the velocity of the outermost zone. Right: Same as left figure, except that the upper curves are LEOS without Maxwell construction, and the lower curves are with the Maxwell construction.

6. Discussion and conclusion

It is evident from figures 2 and 3 that widely spaced wavelength pyrometry measurements of expanding foils will differ at the 15 to 25% level, between the two equations of state (QEOS and LEOS) that have differences as shown in Fig. 1. The brightness temperature is lower at lower frequencies and the pulse duration is longer. It is also worth noting that the choice of whether to use the Maxwell construction in hydrodynamic simulations also makes significant and measurable differences to predicted pyrometry measurements, particularly in the IR for these parameters. The choice of which construction to use is non-trivial. Maxwell construction implies equilibrium has occurred over the length scale of the simulation zone, even in the dynamically changing situation of a rapidly expanding foil. Simulation without the Maxwell construction implies that droplets and bubbles are well resolved, which is unlikely to be true at all scales [15]. For the velocity measurements, the differences between EOS (and between simulations with and without Maxwell construction) are most clearly seen in the longer wavelength results; the differences are on the 10% level for the two candidate EOS's.

We should point out that these calculations have neglected any absorption through the medium and any differences between the propagation of the two polarization states, and so are really only a first look at the ability of NDCX II to clarify EOS questions. We have also used a solid target as the most rigorous test, as the hydrodynamic time scale for this case is the shortest relative to the pulse duration of NDCX II. Including these additional physics and a wide range of materials is currently under study by the authors. Finally we should note that these calculations can also be applied to (and were partially motivated by) laser heated targets if there is initial temperature equilibration followed by hydrodynamic expansion [16].

7. References

1. B.G. Logan, et al., IFSA 2007, Journal of Physics, Conference Series 112 (2008) 032029.
2. N.A. Tahir, et al, Nuclear Instruments and Methods in Physics Research B 245 (2006) 85–93.
3. J.J. Barnard, et al., Proc. 2005 Particle Accelerator Conference, p. 2568 (2005).
4. F.M. Bieniosek, et al, Nucl. Instrum. Meth. A 606 (2009) 146-151.
5. P.A. Seidl, et al, Nucl. Instrum. Meth. A 606 (2009) 75-82.
6. A. Friedman *et al*., Nucl. Instr. and Meth. A **606**, 6 (2009).
7. S. F. Ng, J. J. Barnard, P. T. Leung, B.G. Logan, and S. S. Yu, in preparation (2009).
8. J. J. Barnard, et al, Nuclear Instruments and Methods in Physics Research A, **606**, 134-138, (2009)
9. A. B. Zylstra, J.J. Barnard, and R. M. More, submitted (2009).
10. S. F. Ng, S. Veitzer, J. J. Barnard, P. T. Leung, S. S. Yu, in preparation (2009).
11. B. G. Logan, L. J. Perkins, and J. J. Barnard, Phys. Plasmas **15**, 072701 (2008).
12. J. J. Barnard, et al, Nuclear Instruments and Methods in Physics Research A, 577 (2007) 275-283.
13. R. More, K.H. Warren, D.A. Young, G. B. Zimmerman, Phys. Fluids, **31**, 3062 (1988).
14. P.A. Ni, et al, Laser and Particle Beams, December 2008.
15. J. Armijo and J.J. Barnard, in preparation (2009).
16. P. A. Ni, F. M. Bieniosek, M. Leitner, C. Weber, W. L. Waldron, Nuclear Instruments and Methods in Physics Research A, **606**, (2009), 169-171.